Phytic acid derived bioactive CaO–P$_2$O$_5$–SiO$_2$ gel-glasses

Ailing Li · Dong Qiu

Abstract The possibility of using phytic acid as a precursor to synthesize CaO–P$_2$O$_5$–SiO$_2$ glasses by sol–gel method has been explored and the pseudo ternary phase diagram has been established. It was shown that gel-glasses over a broader range of compositions could be prepared compared to other phosphorus precursors or melt-quenching method. Furthermore, phytic acid was found to assist calcium being incorporated into glass networks. In vitro tests in simulated body fluid (SBF) were performed on the above gel–glasses and it was found that they were bioactive over a much broader compositional range especially at high phosphate content, thus enabling one to design bioactive materials with various degradation rates by adjusting the phosphate content.

1 Introduction

It has been around 40 years since bioactive glass was first introduced in early 1970s by Hench et al. The first quaternary bioactive glass-45S5 Bioglass®, which is composed of 45% SiO$_2$, 24.5% CaO, 6% P$_2$O$_5$ and 24.5% Na$_2$O (mol%), is known to develop an interfacial bond between the implant and surrounding tissues [1]. This material was prepared by melt-quenching method at temperatures between 1,300 and 1,450°C [2]. The rapid formation of hydroxyl carbonate apatite (HCA) exhibited by Bioglass® at the interface with body fluids was attributed to the presence of Na$_2$O and other alkali ions in the glass network [3]. Studies by Ohtsuki [4] and Hench et al. [1] also showed that melt-quenched glasses with more than 60 mol% silica were biologically inactive.

In 1992, it was showed by Li et al. that CaO–P$_2$O$_5$–SiO$_2$ ternary glass (60 mol% SiO2, 36 mol% CaO and 4 mol% P$_2$O$_5$-termed as 58S) produced by a sol–gel technique was no less bioactive than the 45S5 Bioglass® [5]. It also showed higher dissolution rate than 45S5 Bioglass® probably due to its large specific surface area [6, 7]. Furthermore, by this sol–gel route, the highest SiO$_2$ content for bioactive composition can be increased from 60 mol% in those melt-quenched glasses up to 85 mol% [5]. It was shown by Kokubo et al. that phosphate in the glass was only to aid in the nucleation of Ca–P phase on the surface but was not an essential constituent because the surface could adsorb phosphate ions from the body fluid and incorporate them into the HCA layer [8–10]. Saravanapavan and Hench [11] then reported that binary calcium silicate glasses produced by a sol–gel method could be bioactive with SiO$_2$ content up to 90 mol%. The binary gel-glass composed of 70 mol% SiO$_2$ and 30 mol% CaO (named as S70C30) appeared to be the most bioactive compared to all the other binary glasses studied, with a bioactivity no less than 58S and 45S5 [12].

Compared to melt-quenching method, sol–gel routes generally offer low-temperature processing along with the homogenous mixing of the reactants, leading to better quality glasses with easily controlled morphologies [13, 14]. More importantly, from the above examples, one can see that the bioactive compositional range can be significantly altered when using sol–gel methods, for example, the SiO$_2$ content can be dramatically increased. It was found that a significant proportion of surface hydroxyl was present in the sol–gel materials, which might be the reason for bioactivity

A. Li · D. Qiu (✉)
Beijing National Laboratory for Molecular Sciences,
State Key Laboratory of Polymer Physics and Chemistry,
Institute of Chemistry, Chinese Academy of Sciences,
Beijing 100190, China
e-mail: dqiu@iccas.ac.cn

A. Li
Graduate University of Chinese Academy of Sciences,
Beijing 100049, China

in high SiO_2 content glasses [15]. In sol–gel method, different precursors may have different reactivity, thus affecting the final structure and property of resultant gel–glasses [16–20]. So far, in $CaO–P_2O_5–SiO_2$ ternary glasses, the bioactive region has not exceeded the 20 mol% P_2O_5 limit for either melt-quenched or sol–gel derived materials [4, 21]. Given the good biocompatibility and bioresorbability of phosphate materials, increasing P_2O_5 content in bioactive materials certainly has many technical advantages, e.g. better control on dissolution rates [22]. We envisage that by choosing different phosphorus precursors, it is possible to extend the bioactive composition of $CaO–P_2O_5–SiO_2$ ternary systems into higher P_2O_5 content region.

In this study, phytic acid is used in the sol–gel synthesis, and its influences on the glass forming and bioactivity of the resultant $CaO–P_2O_5–SiO_2$ gel–glasses will be extensively examined. Phytic acid (inositol hexakisphosphate, IP6) is non-toxic and has good solubility and stability in the mixture of water and ethanol. In a previous study, we have succeeded in preparing binary $P_2O_5–SiO_2$ materials with high phosphate content (higher than 50 mol% P_2O_5) by a sol–gel method with phytic acid as a precursor in a mixture of water and ethanol [23]. Furthermore, it is worth mentioning that when calcium nitrate, the most common calcium precursor, toxic calcium nitrate does not disappear before calcined at 450°C or above[15]. Given the high affinity of calcium ions with phytic acid, we hope that calcium can be incorporated into the phosphosilicate network at relatively lower temperatures, thus overcoming this long existing problem.

2 Materials and methods

2.1 Materials and synthesis route

The following precursors were used without further purification in the sol–gel preparation. Phytic acid (50 wt% aqueous solution) was purchased from Sigma Aldrich. Tetraethylorthosilicate (TEOS, $\geq$ 99.0%) and $Ca(NO_3)_2\cdot 4H_2O$ were purchased from Sinopharm Chemical Reagent Co., Ltd.

The sol–gel preparation is outlined in Scheme 1. Phytic acid was firstly mixed with ethanol and water at ambient temperature, then TEOS was added through a syringe under magnetic stirring. After 1 h, $Ca(NO_3)_2\cdot 4H_2O$ powder was added under stirring until a transparent solution was formed (the sol). The sols were sealed in polypropylene containers and left to gel. The resultant gels were aged at ambient temperature for 2 days then dried in an oven, firstly at 60°C for 1 week and then at 120°C for another 2 weeks. The dry gels were further heated to 400°C to obtain gel–glasses at a rate of 5°C min^{-1} in air, and then

dwelt at that temperature for 1 h. As all the processing temperatures were far below the componental oxides' boiling temperature, the resultant Ca–P–Si ratios were almost identical to the initial reactant ratios, as confirmed by elemental analysis. Thus in the following text, the gels and gel-glasses are denoted in the form of componental oxides as $(CaO)_x(P_2O_5)_y(SiO_2)_z$, where x, y, and z are the molar fractions of the corresponding oxides, respectively.

2.2 Thermogravimetric analysis (TGA)

Thermal gravimetric behaviors of these gels were measured on a TA Q-600 instrument. The samples (around 5 mg each) were placed in alumina crucibles and measured under nitrogen flow at 20 ml min^{-1}. Data were collected from 50 to 800°C at a heating rate of 5°C min^{-1}.

2.3 X-ray diffraction study (XRD)

Samples for XRD measurements were finely powderised and measured on a Rigaku (D/MAX 2500) instrument with Cu Kα radiation ($\lambda = 1.54$Å), operated at 40 kV and 200 mA. The data were collected at 2θ from 5 to 70° by 4°min^{-1}.

2.4 Scanning electron microscopy (SEM) and energy disperse X-ray spectroscopy (EDXS)

Samples for SEM measurements were coated with a thin layer of gold (Au) by sputtering (SCD 500) and then the microstructures of the surface were observed on a Hitachi (4,800) instrument coupled with EDXS at an acceleration voltage of 15 kV.

2.5 Bioactivity test

Bioactivities were tested in vitro by reacting the samples with simulated body fluid (SBF) at 36.5 ± 0.5°C as
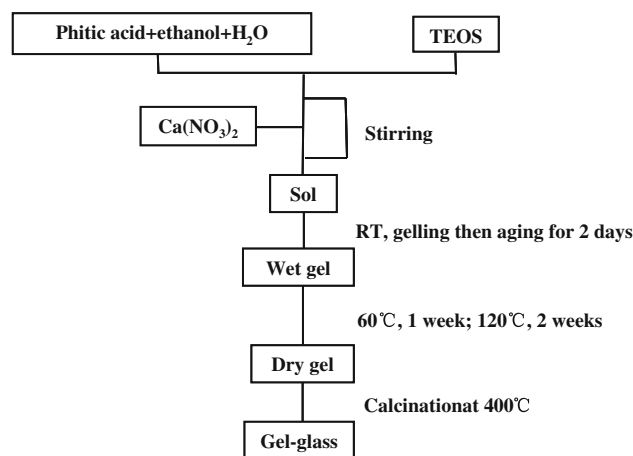
Scheme 1 Flow diagram of the sol–gel preparation process

described elsewhere [24]. Hydroxylapatite (HA) formation was monitored by SEM, EDXS and XRD. SBF has almost identical ion concentrations to those of the human blood plasma (HBP) as shown in Table 1.

3 Results

Figure 1 shows the pseudo ternary phase diagram of the sol–gel process; the gelling/non–gelling boundary is indicated by a solid line. The gelling time varies substantially with the initial sol compositions, from 1 day to 4 weeks. Generally, the gelling rate increases with the decrease in SiO_2 content; however, no gels were formed when silica content was lower than c.a. 18 mol% within the experimental timescale. The ratio between P_2O_5 and CaO does not affect the phase boundary too much.

Figure 2 shows TGA traces of representative gels, after dried at 120°C. The weight losses for all samples are similar. Two stages of weigh loss were observed: the first one occurred between 200 and 250°C, which may be associated with the removal of trapped solvent (water and ethanol etc.). More weight loss commenced from the end of first weight loss (~ 250°C) up to ~ 600°C, which is most likely due to the loss of organic moieties by further condensation. The maximum weight loss rate takes place between 300 and 400°C, thus the gels were further calcined at 400°C to remove organic residuals; the weight loss above that may due to the elimination of hydroxyls. It can also be seen from Fig. 2 that the weight losses increase with the increase in P_2O_5 content (from 25 to 56 mol%), possibly reflecting a higher hydroxyl content associated with the more hydroscopic phosphates. In general, the dried gels showed overall weight losses around 20–30% over the temperature range 50–800°C during the course of TGA measurements.

As degradable biomedical materials for implants, amorphous materials are desired because they are isotropic thus do not produce fragments during the degradation (fragmental pieces usually cause inflammation). XRD was used to check the crystallographic features of these gels. Firstly, the gels after dried at 120°C for 2 weeks were examined. Generally, with the increase in CaO content the samples become crystalline (Fig. 3). The crystalline phases was identified as mainly $CaPO_3(OH)$ (Fig. 3d) first, then
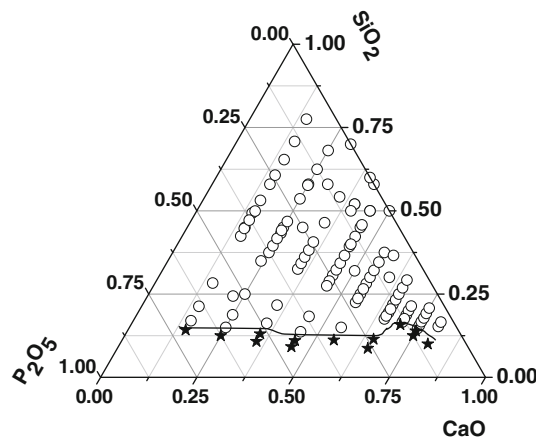

Fig. 1 Pseudo phase diagram of the phytic acid-TEOS-Ca(NO₃)₂ ternary mixtures. *circle* gelling; *star* non-gelling. The gelling/non-gelling boundary is indicated by a *solid line*
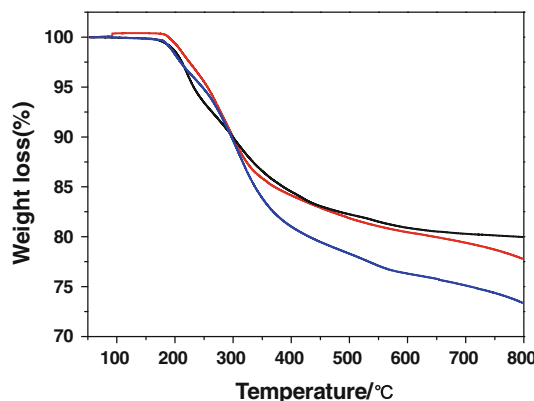

Fig. 2 The TGA traces of the calcium phosphosilicate gels. *Top* $(CaO)_{0.25}(SiO_2)_{0.50}(P_2O_5)_{0.25}$, *middle* $(CaO)_{0.26}(SiO_2)_{0.37}(P_2O_5)_{0.37}$, *bottom* $(CaO)_{0.25}(SiO_2)_{0.19}(P_2O_5)_{0.56}$

$Ca(NO_3)_2$, the residual calcium precursor, with further increasing CaO content. At a fixed CaO content, with the increase in P_2O_5 content, samples become amorphous again (Fig. 4). Interestingly, with the decrease in P_2O_5 content, the major crystalline phases also turned from $CaPO_3(OH)$ into $Ca(NO_3)_2$ (Fig. 4a – c). Detailed pseudo phase diagram is shown in Fig. 5.

The as-obtained dried gels need to be further calcined in order to produce gel-glasses. According to the TGA results, 400°C was chosen because most of the organic moieties can be removed but no crystallization takes place at this

Table1 Ion concentrations of HBP and SBF

	Ion concentration (mM)							
	Na^+	K^+	Mg^{2+}	Ca^{2+}	Cl^-	HCO_3^-	HPO_4^{2-}	SO_4^{2-}
HBP	142.0	5.0	1.5	2.5	103.0	27.0	1.0	0.5
SBF	142.0	5.0	1.5	2.5	147.8	4.2	1.0	0.5
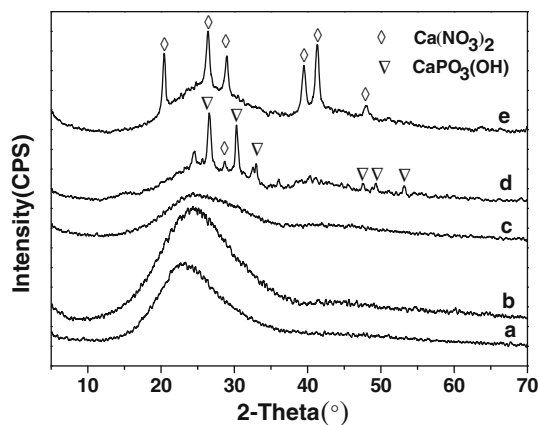
Fig. 3 XRD spectra of representative CaO-SiO$_2$-P$_2$O$_5$ (P$_2$O$_5$/SiO$_2$ = 0.4, molar ratio) samples after dried at 120°C for two weeks at different CaO molar fractions. (*a*) 0.15; (*b*) 0.25; (*c*) 0.35; (*d*) 0.45; (*e*) 0.55

Fig. 4 XRD spectra of representative CaO-SiO$_2$-P$_2$O$_5$ (CaO = 0.55, molar fraction) samples after dried at 120°C for 2 weeks at different P$_2$O$_5$/SiO$_2$ ratios. (*a*) 0.29; (*b*) 0.50; (*c*) 0.67; (*d*) 1.0; (*e*) 2.0

temperature. Since we are mainly interested in amorphous materials, only those being amorphous at 120°C were further calcined. As expected, all the amorphous gels remained amorphous after calcination at 400°C (Fig. 6). Thus in Fig. 5, the amorphous region can also be viewed as the gel-glass formation region.

The as-formed gel–glasses were soaked in SBF to test their bioactivity. Figure 7 gives the XRD spectra of three representative gel-glasses covering different compositional ranges, before and after reacting with SBF. For the sample (CaO)$_{0.35}$(SiO$_2$)$_{0.54}$(P$_2$O$_5$)$_{0.11}$, over the amorphous background, Bragg peaks of HA were evident after soaked in SBF for 14 days, indicating excellent bioactivity. The XRD spectra also showed an evolution of apatite formation upon reacting with SBF for various spells. It is interesting to find that although apatite signals increases with soaking time in SBF, it does not change after 14 days (Fig. 8). Therefore, 14 days was chosen as the critical time for apatite forming investigation. For the sample (CaO)$_{0.26}$(SiO$_2$)$_{0.37}$(P$_2$O$_5$)$_{0.37}$, both Bragg peaks of HA and Ca(H$_2$PO$_4$)$_2$ were detected after immersed in SBF for 14 days; given the good biocompatibility of Ca(H$_2$PO$_4$)$_2$, this sample could still be viewed as bioactive. However, the sample (CaO)$_{0.15}$(SiO$_2$)$_{0.53}$(P$_2$O$_5$)$_{0.32}$ remained amorphous and almost unchanged after 14 days, indicating a lack of bioactivity.

The surface morphology of gel-glass (CaO)$_{0.35}$(SiO$_2$)$_{0.54}$(P$_2$O$_5$)$_{0.11}$ was also examined by SEM-EDXS (Fig. 9). Before soaked in SBF, the micrograph showed a smooth surface characteristic of a nonporous and homogeneous gel. Also, EDXS confirmed Si, P and Ca as the main componental constitutes. The micrograph of the glass after 14 days showed the monolith surface partially covered by a layer of spherical particles. A higher magnification micrograph (Fig. 9b, inset) revealed that these particles were aggregates of numerous needle-shaped crystallites, which are the characteristic of apatite phase grown over
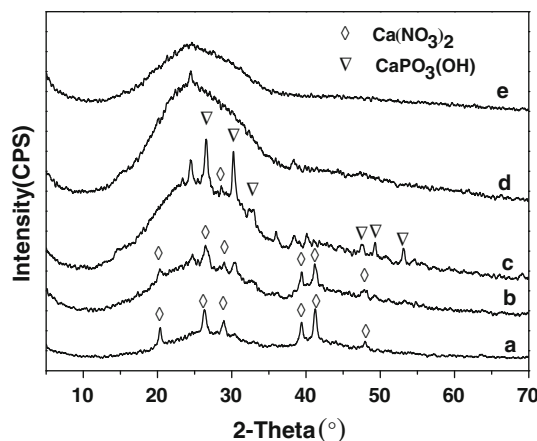

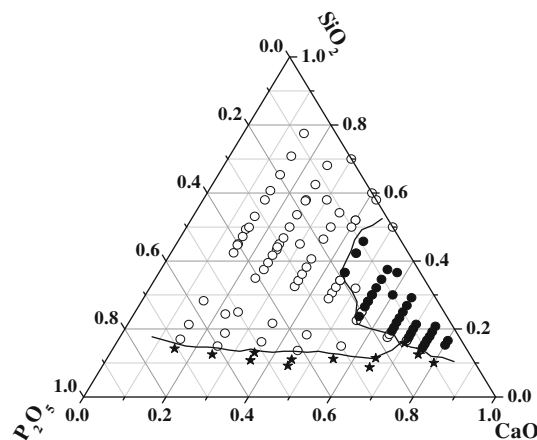**Fig. 5** Composition dependence of CaO-SiO$_2$-P$_2$O$_5$ gel crystallization. The boundaries are illustrated by *solid lines. circle* amorphous; *filled black circle* crystalline, *star* non-gelling

bioactive material surfaces. The EDXS analysis also indicated that Ca and P contents increased (Ca/P $\sim$1.67), accompanied by a dramatic decrease in the concentration of Si, supporting the development of an extended apatite layer on the surface. Indeed, the Si content was so low, indicating that the apatite layer was considerably thick. Therefore, these SEM-EDXS results are also in good agreement with the XRD results (Fig. 7b). In the region where SiO$_2$ content is low while P$_2$O$_5$ content is high, samples dissolved severely in SBF (some samples even dissolved within 10 min); therefore no further analysis of apatite forming was performed on these samples. Generally, the overall dissolution rate increases with P$_2$O$_5$/SiO$_2$ ratio. Interestingly, in the region where CaO molar fraction is lower than 0.4 and P$_2$O$_5$ molar fraction is between 0.25 and 0.4, the gel–glasses did not show any bioactivity even after soaked in SBF for 6 weeks. Other gel–glasses all showed bioactivity within 14 days soaked in SBF. The in
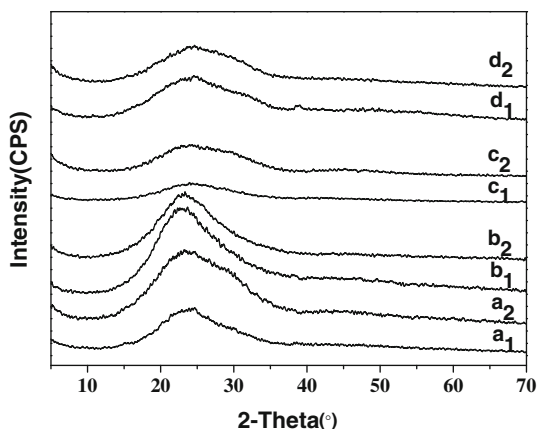
Fig. 6 XRD spectra of representative CaO-P_2O_5-SiO_2 gels dried at 120°C (with *subscript 1*) and the gel-glasses obtained from calcination at 400°C (with *subscript 2*). (*a*) $(CaO)_{0.25}(SiO_2)_{0.50}(P_2O_5)_{0.25}$; (*b*) $(CaO)_{0.15}(SiO_2)_{0.50}(P_2O_5)_{0.35}$; (*c*) $(CaO)_{0.25}(SiO_2)_{0.62}(P_2O_5)_{0.13}$; (*d*) $(CaO)_{0.45}(SiO_2)_{0.14}(P_2O_5)_{0.41}$
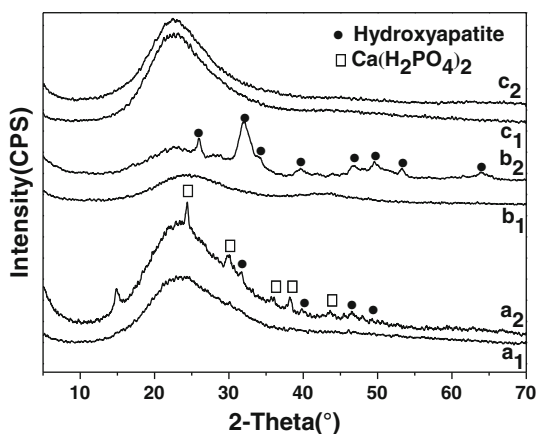

Fig. 7 XRD spectra of three representative gel-glass before (with *subscript 1*) and after (with *subscript 2*) reacting with SBF for 14 days. (*a*) $(CaO)_{0.26}(SiO_2)_{0.37}(P_2O_5)_{0.37}$; (*b*) $(CaO)_{0.35}(SiO_2)_{0.54}(P_2O_5)_{0.11}$; (*c*) $(CaO)_{0.15}(SiO_2)_{0.53}(P_2O_5)_{0.32}$
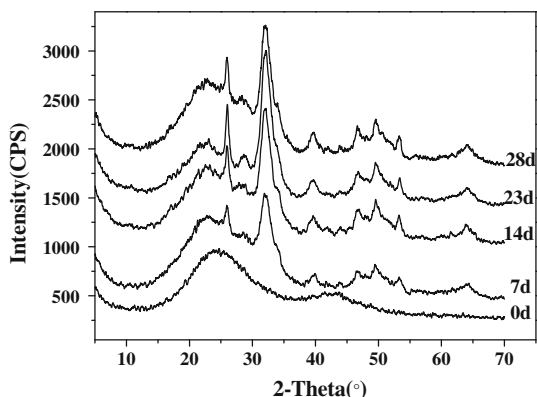

Fig. 8 The evolution of XRD spectra of gel-glass (CaO)$_{0.35}$(SiO$_2$)$_{0.54}$(P$_2$O$_5$)$_{0.11}$ upon reacting with SBF for various spells

vitro behavior of the sol–gel derived CaO–P_2O_5–SiO_2 samples is summarized in Fig. 10.

4 Discussion

In this study, it is apparent that the phosphorus precursor (phytic acid) plays an important role in the production of CaO–SiO_2–P_2O_5 glasses by sol–gel method. Phytic acid itself is non-toxic and the co-solvent has low toxicity, making this preparation route very promising for biomedical applications [25]. It is clear that phytic acid can form gels with TEOS and Ca(NO$_3$)$_2$. The gelling rate increases with P_2O_5/SiO_2 (molar ratio), probably due to the self-catalysis of phytic acid towards hydrolysis and condensation in sol–gel process [26]. As mentioned earlier, when calcium nitrate was used as calcium precursor, high percentages of calcium nitrate were found in the dried gels unless calcined at a temperature higher than 450°C [15]. With phytic acid involved, this situation had been largely improved. Most of the dried gels were amorphous and no calcium nitrate signals were detected by XRD even only treated at 120°C (Fig. 6), which might be owing to the good affinity of phytic acid to calcium ions, facilitating the breaking down of calcium nitrate. However, from Figs. 3 and 4, one can see that at higher CaO content and lower P_2O_5 content, gels were crystalline, where calcium nitrate signals were observed. This observation again supports the key role of phytic acid in assisting calcium to enter the gel network. A detailed study on the calcium local environment on these samples is still undergoing in our group using Ca k-edge XANES. The presence of crystalline CaPO$_3$(OH) in some compositions might be due to the reaction of phytic acid with calcium nitrate. With the increase in P_2O_5 content or decrease in CaO content, the crystalline phases disappeared, suggesting a possible stoichiometric event between phytic acid and calcium nitrate. From the above observations, it is clear that phytic acid is a good phosphorus precursor, which not only enables the production of calcium phosphosilicate gels over a wide composition range, but also helps the incorporation of calcium into gel networks at relatively low temperatures. The absence of toxic calcium nitrate also opens a possibility for the dried gels to be used directly as implants in some circumstances, thus some thermally unstable active species (e.g. antibiotics) could be loaded in the gels in situ. After calcined at 400°C, gel–glasses were formed over a broad composition region, again probably due to the good compatibility of phytic acid with both Si and Ca precursors.

Besides the improvements in the sol–gel process and glass forming of CaO–SiO_2–P_2O_5, the gel–glasses derived from phytic acid also showed bioactivity over a wider composition range (Fig. 10) and better resistance to

Fig. 9 SEM micrographs and EDXS spectra of the gel-glass $(CaO)_{0.35}(SiO_2)_{0.54}(P_2O_5)_{0.11}$ before (**a**) and after (**b**) soaked in SBF for 14 days

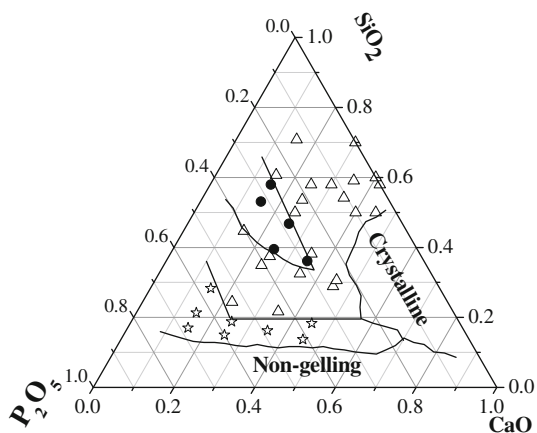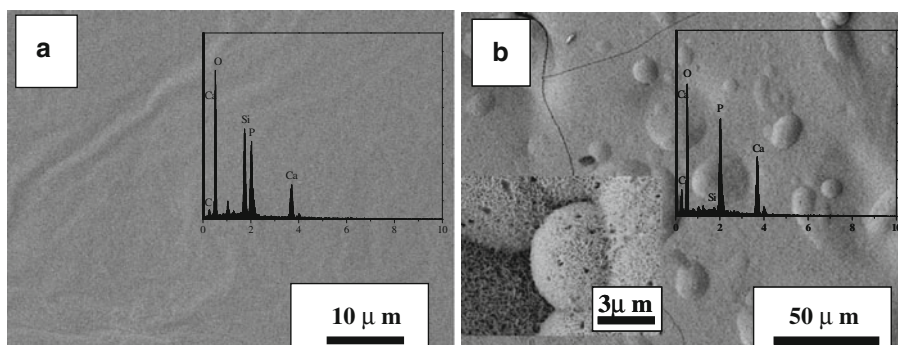**Fig. 10** Composition dependence of the bioactive $CaO–SiO_2–P_2O_5$ gel–glasses. *Triangle* HA formation, *filled black circle* no HA formation, *star* dissolution

content. It is not clear at this stage for the reason of these changes, but it might be related to the high affinity of phytic acid with calcium ions, which may result in a calcium distribution mainly around phosphate tetrahedrons and an effective increase of Ca/P ratio [27], or due to the presence of octahedral silicate as shown in a previous study [23], which might be more reactive towards hydrolysis. Further investigation on the local environment of componential elements is still undergoing with solid state MAS-NMR and X-ray absorption spectroscopy. The bioactivity at high phosphate content is especially interesting, which can facilitate the designing of biomedical materials with controllable degrading rate since phosphate glasses generally degrade much faster than silicate glasses [22]. The degradation rate of these gel–glasses shall be adjustable from a few days (high phosphate content) to a few years (pure silicate), meeting with the requirement of different terminal applications, such as controlled drug release or bone replacement.

5 Conclusions

Phytic acid was used as the phosphorus precursor to prepare $CaO–SiO_2–P_2O_5$ glasses by a sol–gel process. Phytic acid showed good compatibility with both Si (TEOS) and Ca precursors (calcium nitrate) in a mixture of low-toxic ethanol and water. It was found that phytic acid helped calcium to enter the gel network without the need of further calcinations. The obtained gel–glasses showed bioactivity at high phosphate content region compared to those made from melt-quenching or sol–gel methods from other phosphorus precursors. The commence of bioactivity at high P_2O_5 content provides better control over the overall dissolution rate of $CaO–P_2O_5–SiO_2$ ternary systems thus meeting with the requirements of various terminal biomedical applications.

dissolution than previously reported similar materials prepared by either melt-quenching or sol–gel methods from other phosphorus precursors [4, 21]. Ohtsuki et al. [4] studied the behavior of melt-quenched $CaO–P_2O_5–SiO_2$ ternary systems in detail. It was found that there were two glass formation regions. Glasses containing no or a small amount of P_2O_5, such as the composition of $(CaO)_{0.40}(SiO_2)_{0.60}$, $(CaO)_{0.48}(P_2O_5)_{0.03}(SiO_2)_{0.49}$ and $(CaO)_{0.61}(P_2O_5)_{0.09}(SiO_2)_{0.30}$ formed an apatite layer on their surfaces in SBF. Whereas glasses with high P_2O_5 content such as $(CaO)_{0.20}(P_2O_5)_{0.40}(SiO_2)_{0.40}$, $(CaO)_{0.32}(P_2O_5)_{0.50}(SiO_2)_{0.18}$ and $(CaO)_{0.41}(P_2O_5)_{0.44}(SiO_2)_{0.15}$ were severely dissolved in SBF and did not form HA. Other regions were non-glass-forming region (see [4] for detail). The sol–gel derived $CaO–P_2O_5–SiO_2$ when using other phosphorus precursors showed different performances towards bioactivity, notably in the shifting of bioactive region boundary towards higher SiO_2 content, but still showing no obvious change in the dependence on P_2O_5 content [21]. On the contrary, the sol–gel $CaO–P_2O_5–SiO_2$ ternary systems studied in this work are very different from those previous reports when reacting with SBF, notably in the decreased dissolution rate and commence of bioactivity at high P_2O_5

References

1. Hench LL, Splinter RJ, Allen WC, Greenlee TK Jr. Bonding mechanisms at the interface of ceramic prosthetic materials. J Biomed Mater Res. 1971;2:117–41.
2. Hench LL. The story of bioglass (R). J Mater Sci Mater Med. 2006;17:967–78.
3. Hench LL, Andersson O. Introduction to bioceramics. In: Hench LL, Wilson J, editors. Bioactive glasses. Singapore: World Scientific; 1993. p. 41.
4. Ohtsuki C, Kokubo T, Takatsuka K, Yamamuro T. Compositional dependence of bioactivity of glasses in the system CaO-SiO2–P2O5: its in vitro evaluation. Nippon Seramikkusu Kyokai Gakujutsu Ronbunshi. 1991;99:1–6.
5. Li R, Clark AE, Hench LL. Effects of structure and surface area on bioactive powders by sol–gel process. Chem Pro Adv Mater. 1992;56:627–33.
6. Hamadouche M, Meunier A, Greenspan DC, Blanchat C, Zhong JPP, La Torre GP, Sedel L. Long-term in vivo bioactivity and degradability of bulk sol–gel bioactive glasses. J Biomed Mater Res. 2001;54:560–6.
7. Greenspan DC, Zhong JP, Wheele DL. Bioactivity and biodegradability: melt versus sol–gel derived glasses in vitro and in vivo. In: LeGeros RZ, LeGeros JP, editors. Bioceramics 11. 1998. p. 348.
8. Ebisawa Y, Kokubo T, Ohura K, Yamamuro T. Bioactivity of CaO–SiO2 based glasses in vitro evaluation. J Mater Sci Mater Med. 1990;1:239–44.
9. Ohura K, Nakamura T, Yamamuro T, Kokubo T, Ebisawa Y, Kotoura Y, Oka M. Bone-bonding ability of P2O5-free CaO·SiO2 glasses. J Biomed Mater Res. 1991;25:357–65.
10. Kokubo T. A/W glass-ceramics: processing and properties. In: Hench LL, Wilson J, editors. Introduction to bioceramics. Singapore: World Scientific; 1993. p. 75.
11. Pereira MM, Hench LL. Mechanisms of hydroxyapatite formation on porous gel-silica substrates. J Sol Gel Sci Technol. 1996;7:59–68.
12. Saravanapavan P, Jones JR, Verrier S, Beilby R, Shirtliff VJ, Hench LL, Polak JM. Binary CaO–SiO2 gel-glasses for biomedical applications. Bio-Med Mater Eng. 2004;14:467–86.
13. Li N, Jie Q, Zhu SM, Wang RD. Preparation and characterization of macroporous sol–gel bioglass. Cera Inter. 2005;31:641–6.
14. Arcos D, Vallet-Regi M. Sol–gel silica-based biomaterials and bone tissue regeneration. Acta Biomater. 2010;6:2874–88.
15. Lin S, Ionescu C, Pike KJ, Smith ME, Jones JR. Nanostructure evolution and calcium distribution in sol–gel derived bioactive glass. J Mater Chem. 2009;19:1276–82.
16. Carta D, Pickup DM, Knowles JC, Smith ME, Newport RJ. Sol–gel synthesis of the P2O5–CaO–Na2O–SiO2 system as a novel bioresorbable glass. J Mater Chem. 2005;15:2134–40.
17. Pickup DM, Guerry P, Moss RM, Knowles JC, Smith ME, Newport RJ. New sol–gel synthesis of a $(CaO)_{0.3}(Na2O)_{0.2}(P2O5)_{0.5}$ bioresorbable glass and its structural characterization. J Mater Chem. 2007;17:4777–84.
18. Saboori A, Rabiee M, Moztarzadeh F, Sheikhi M, Tahriri M, Karimi M. Synthesis, characterization and in vitro bioactivity of sol-gel-derived SiO2–CaO–P2O5–MgO bioglass. Mater Sci Engi C. 2009;29:335–40.
19. Balamurugan A, Balossier G, Kannan S, Michel J, Rebelo AHS, Ferreira JMF. Development and in vitro characterization of sol–gel derived CaO–P2O5–SiO2–ZnO bioglass. Acta Biomater. 2007;3:255–62.
20. Zhang L, Eckert H. Synthesis and structural evolution of Al2O3–B2O3–P2O5 gels and glasses. J Mater Chem. 2005;15:1640–53.
21. Hench LL. Biomaterials: a forecast for the future. Biomaterials. 1998;19:1419–23.
22. Abou Neel EA, Pickup DM, Valappil SP, Newport RJ, Knowles JC. Bioactive functional materials: a perspective on phosphate-based glasses. J Mater Chem. 2009;19:690–701.
23. Qiu D, Guerry P, Knowles JC, Smith ME, Newport RJ. Formation of functional phosphosilicate gels from phytic acid and tetraethyl orthosilicate. J Sol Gel Sci Technol. 2008;48:378–83.
24. Kokubo T, Takadama H. How useful is SBF in predicting in vivo bone bioactivity. Biomaterials. 2006;27:2907–15.
25. Munoz JA, Valiente M. Determination of phytic acid in Urine by inductively coupled plasma mass spectrometry. Anal Chem. 2003;75:6374–8.
26. Samba-Fouala C, Mossoyan JC, Mossoyan-Deneux M, Benlian D, Chaneac C, Babonneau F. Preparation and properties of silica hybrid gels containing phytic acid. J Mater Chem. 2000;10:387–93.
27. Li A, Wang D, Xiang J, Newport RJ, Reinholdt MX, Mutin PH, Vantelon D, Bonhomme C, Smith ME, Laurencin D, Qiu D. Insights into new calcium phosphosilicate xerogels using an advanced characterization methodology. J Non Crystal Solids. 2011;357:3548–55.